Pre-Registration for Improved Latent Fingerprint Identification

Ram P. Krish, Julian Fierrez,
Daniel Ramos, Javier Ortega-Garcia
Biometric Recognition Group - ATVS
EPS - Universidad Autonoma de Madrid
28049 Madrid, Spain.
{*ram.krish, julian.fierrez, daniel.ramos, javier.ortega*}*@uam.es*

Josef Bigun
Intelligent Systems Laboratory
Halmstad University
Box 823 SE-30118
Halmstad, Sweden
josef.bigun@hh.se

***Abstract*—Comparing a latent fingerprint minutiae set against a tenprint fingerprint minutiae set using an automated fingerprint identification system is a challenging problem. This is mainly because latent fingerprints obtained from crime scenes are mostly partial fingerprints, and most automated systems expect approximately the same number of minutiae between query and the reference fingerprint under comparison for good performance. In this work, we propose a methodology to reduce the minutiae set of tenprint with respect to that of query latent minutiae set by registering the orientation field of latent fingerprint with the tenprint orientation field. By reducing the search space of minutiae from the tenprint, we can improve the performance of automated identification systems for latent fingerprints. We report the performance of our registration algorithm on the NIST-SD27 database as well as the improvement in the Rank Identification accuracy of a standard minutiae-based automated system.**

I. Introduction

Minutiae-based representation is the widely accepted representation by many automated fingerprint matching systems. It is also significant because of its strict analogy with the forensic friction ridge analysis [1]. The minutia-based decision is accepted as a proof of identity legally by courts in almost all countries around the world [2].

Automated Fingerprint Identification Systems (AFIS) in general assume approximately the same size of minutiae set between the query and reference minutiae for identification accuracy [3]. It is nevertheless frequent in some scenarios to have very different sizes between query and reference.

Partial fingerprints can arise in a number of situations, for example [3] [4]:

- the unintentional traces of the fingerprint left by the perpetrator in a crime scene (*latent* fingerprints are mostly partial in nature).
- due to small size of the fingerprint capturing/acquisition devices (compact silicon-chip based sensors).
- an already enrolled/acquired fingerprint has noisy regions and is left only with a partial good/recognizable region for identification.

The performance of the existing partial fingerprint identification systems/algorithms mainly depends on the image quality, the number of minutia available and other derived and extended features that can be obtained from the partial fingerprint region. Various approaches in partial fingerprint identification [4] include the use of localized secondary features derived from relative minutia information [3], using representative points along ridge lines in addition to minutiae [5] and use of Level-3 features such as dots and incipients [6].

To improve the performance of AFIS in the partial fingerprint comparison scenario, it will be advantageous if we can reduce the minutiae search space of the reference (full fingerprint) with respect to the query (partial fingerprint) minutiae set. One methodology that can be adapted to reduce the minutiae search space of the full fingerprint minutiae set can be to register the orientation field (OF) of partial fingerprint with that of the OF of full fingerprint. We then need to perform minutia comparison only with those minutiae that fall in the subregion of the full fingerprint where the partial fingerprint is registered. Such a registration methodology can yield extra information that can augment minutia-based matching strategies.

In this work, we propose a registration algorithm using the OF of both partial and full fingerprint solely generated from their respective minutia sets as proposed in [7], as well as OF directly estimated from latent and tenprint fingerprint images using gradient based approach [8]. The work by Feng and Jain [7] in reconstructing the fingerprint image from minutia sets alone, and successfully launching attacks against fingerprint recognition system indicates that the fidelity of the reconstructed OF to the actual OF is significant. It was also shown that the performance of the algorithm in reconstructing the OF did not drop much even when only 60% of minutiae are only available for OF reconstruction.

The ability to reconstruct OF with only few minutiae supports the rationale behind using this OF reconstruction technique to perform pre-registration and generate a subset of minutiae from the full fingerprint minutiae set before using the AFIS. This work is an extension of [9], where we first presented a preliminary correlation based OF registration method, using only minutiae for OF generation. In the present work, we also study the effect of OF generated from fingerprint images, and also use this registration as a pre-registration stage to improve the rank identification rate of minutiae-based matcher.

In the following sections, we discuss the database used in the experiments, the similarity measure used in the registration, a detailed description of partial fingerprint registration algorithm, followed by experiments, results, conclusion and future work.

II. Database

NIST Special Database 27 (NIST-SD27) [10] is a publicly available forensic fingerprint database which provides minutia sets for latent and its matching tenprint images. The NIST-SD27 minutia set database is broadly classified into two [10] [11]: 1) *ideal*, and 2) *matched* minutia set database. The *ideal* minutia set for latents was manually extracted by a forensic examiner without any prior knowledge of its corresponding tenprint image. The *ideal* minutiae for tenprints was initially extracted using an AFIS, and then these minutiae were manually validated by at least two forensic examiners. The *matched* minutia set contains those minutiae which are in common between the latent and its mated tenprint image. There is a one-to-one correspondence in the minutiae between the latent and its mate in the matched minutia set. This ground truth (matched minutia set) was established manually by a forensic examiner looking at the images and the *ideal* minutiae.

The NIST-SD27 database consists of latent fingerprints of varying quality. It already contains a classification of the latent fingerprints based on the subjective quality of the image into Good, Bad and Ugly, containing 85, 88 and 85 fingerprints respectively determined by the forensic examiner. In [12], it is shown that there is a correlation between these subjective classification and matching performance.

III. Similarity measure

The space of discrete images of same size taking scalar values is a vector space [13, Chapter 3]. A vector space which has a scalar product defined in itself is called a Hilbert space. Let $\mathbf{U}$ and $\mathbf{V}$ be discrete images of same size, represented as a 2D array where the array elements may represent values of gray pixel (*zero-order tensors*), color pixel (*first-order tensors*) or local directions (*second-order tensors*).

The Schwarz inequality:

$$\frac{|\langle \mathbf{U}, \mathbf{V} \rangle|}{\|\mathbf{U}\| \times \|\mathbf{V}\|} \leq 1 \tag{1}$$

holds for $\mathbf{U}$ and $\mathbf{V}$. Here, $\langle \mathbf{U}, \mathbf{V} \rangle$ is the scalar product between $\mathbf{U}$ and $\mathbf{V}$ calculated as :

$$\langle \mathbf{U}, \mathbf{V} \rangle = \sum_{r,c} \mathbf{U}(r,c)^* \cdot \mathbf{V}(r,c) \tag{2}$$

where r, c are the indices, $\mathbf{U}(r,c)^*$ is the complex conjugate of $\mathbf{U}(r,c)$, and $\|\mathbf{U}\|$ and $\|\mathbf{V}\|$ are the L_2 norms of $\mathbf{U}$ and $\mathbf{V}$ respectively.

The L_2 norm $\|\mathbf{U}\|$ is calculated as:

$$\|\mathbf{U}\| = \left[\sum_{r,c} \mathbf{U}(r,c)^* \cdot \mathbf{U}(r,c) \right]^{1/2} \tag{3}$$

and similarly for $\|\mathbf{V}\|$.

The normalized correlation between $\mathbf{U}$ and $\mathbf{V}$, referred to as Schwarz Similarity (SS) hereafter is defined as:

$$SS(\mathbf{U}, \mathbf{V}) = \frac{|\langle \mathbf{U}, \mathbf{V} \rangle|}{\|\mathbf{U}\| \times \|\mathbf{V}\|} \tag{4}$$

Because of Eq.(1), the interval for SS is in the range $[0, 1]$. By calculating SS as a similarity measure, we can locate a given pattern (a small image) in a large image. When $SS(\mathbf{U}, \mathbf{V})$ is 1, then both $\mathbf{U}$ and $\mathbf{V}$ are viewed as most similar patterns, and when $SS(\mathbf{U}, \mathbf{V})$ is 0, they are least similar [13].

IV. Algorithm

We present the algorithm of partial fingerprint registration using the forensic terminologies for the fingerprint. The partial fingerprint is mentioned as latent, and the full fingerprint is mentioned as tenprint. The algorithm to register the orientation field of the latent fingerprint minutia set with that of the tenprint is detailed as follows:

Step 1: Given a latent minutia set L and a tenprint minutia set T, reconstruct the orientation field from the minutia using the algorithm defined in [7]. This orientation field is in the range $[-90, +90]$ degrees, and can be obtained for 8×8 or 16×16 block size. In our experiments, we used 16×16 block size for the orientation field (see Figs. 1(a), 1(b)). The target of the registration algorithm is to locate the region depicted in Fig. 1(c).

Step 2: Generate the orientation tensors for the latent L and tenprint T in double angle (i.e, in the range $[-180, +180]$ degrees) using complex numbers, as follows:

$$\begin{aligned} \bar{L} &= \exp(i \times 2 \times \theta_L) \\ \bar{T} &= \exp(i \times 2 \times \theta_T) \end{aligned} \tag{5}$$

where i is the complex number $\sqrt{-1}$, θ_L and θ_T are the angles of L and T from Step 1.

The complex field, which depicts the local orientation thus obtained can be viewed as a field of second-order tensors, which in turn is a Hilbert Space. We can find the scalar product between $\bar{L}$ and $\bar{T}_s$, as follows:

$$\langle \bar{L}, \bar{T}_s \rangle = \sum_{r,c} \bar{L}(r,c)^* \cdot \bar{T}_s(r,c) \tag{6}$$

where r, c are the indices, $\bar{L}(r,c)^*$ is the complex conjugate of $\bar{L}(r,c)$ and $\bar{T}_s$ is a subregion of $\bar{T}$ that is of same size as $\bar{L}$ located at a position indexed by s.

Step 3: Define the bounding box for the latent orientation tensors $\bar{L}$ by discarding the background. The bounding box can be estimated by the minimum and maximum row and column numbers that correspond to the foreground of latent orientation tensors, see Fig. 1(d). The orientation field for the tenprint image is shown in Figure 1(e). This $\bar{L}$ in Fig. 1(d) is the pattern that we want to locate in the tenprint $\bar{T}$ in Fig 1(e).

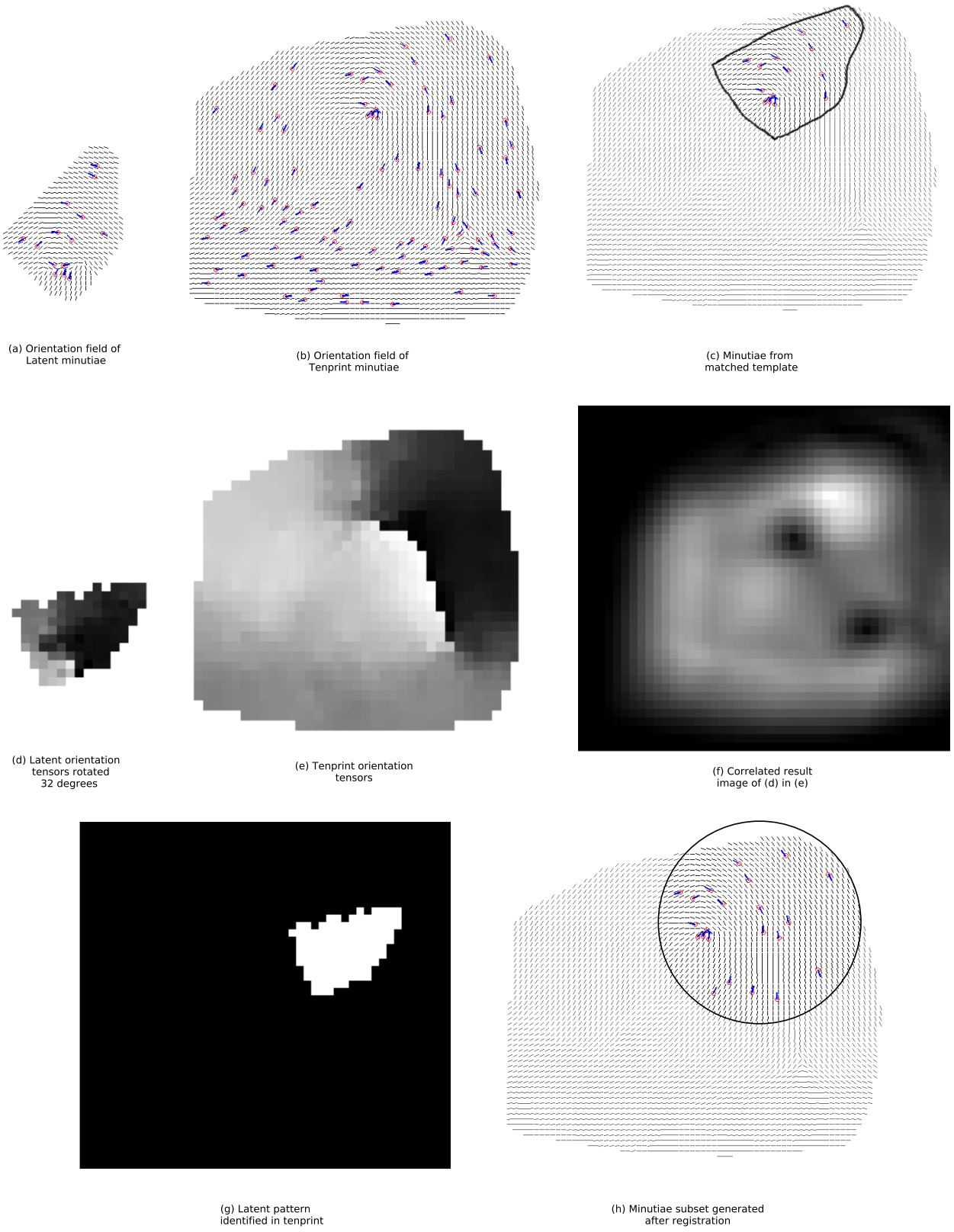

Fig. 1. Various stages in the registration algorithm shown on B101L9 (latent) and B101T9 (tenprint) of NIST-SD27. (a) and (b) are the orientation field (OF) generated from the ideal minutia set, with the minutiae plotted over the OF. (c) is the region in the tenprint that is to be found after registration of (a) into (b), (d) and (e) are the orientation tensors of latent and tenprint. Here (d) is rotated $+32°$. (f) is the result of correlating (d) and (e). (g) is the region were latent pattern is identified in tenprint. (h) is the minutia region selected by our registration algorithm in this example.

Step 4: When searching for the pattern $\bar{L}$ in $\bar{T}$, it is possible that $\bar{L}$ is not perfectly aligned with $\bar{T}$, rotation wise. To compensate for the rotation alignment, we need to test the latent $\bar{L}$ against tenprint $\bar{T}$ for various rotations of $\bar{L}$. In our experiments, we rotate $\bar{L}$ in the range $[-45, +45]$ degrees with a step size $\Delta\theta$ of 1 degree. We denote the rotated $\bar{L}$ as $\bar{L^{\theta}}$. A geometric rotation of the field implies an appropriate rotation of tensor field (complex values) with $2\Delta\theta$.

Step 5: Correlate the conjugate of the latent orientation tensor $\bar{L^{\theta}}^*$ with $\bar{T}$ to generate all possible $\langle \bar{L^{\theta}}, \bar{T_s} \rangle$, the scalar products between $\bar{L^{\theta}}^*$ and $\bar{T_s}$ for varying locations s. The result of this operation can be seen as a complex image indexed by s which is of the size of $\bar{T}$, see Fig. 1(f).

Step 6: From the correlated result, find the point (or index) $s = (r_m^{\theta}, c_m^{\theta})$ where the magnitude of the scalar product is maximum. In [9], the location where phase is minimum was also used. But experimental results show that using only locations of maximum magnitude generates similar results. So, in this work, only location of maximum magnitude is used. Both maximum magnitude and minimum phase convey the region in $\bar{T}$ where $\bar{L^{\theta}}$ agrees the most.

Step 7: Find the similarity based on Schwarz inequality as explained in Section III, between $\bar{L^{\theta}}$ and $\bar{T_s^m}$ centered at $(r_m^{\theta}, c_m^{\theta})$. The L_2 norms $\|\bar{L^{\theta}}\|$ and $\|\bar{T_s^m}\|$ for different θ are equal because the orientation tensors $e^{i2\theta_L}$ and $e^{i2\theta_T}$ are not estimated from the gray pixel gradients, but reconstructed from minutia orientations. Consequently, these orientation tensors are complex numbers falling on a unit circle, representing the local direction. So, the magnitude of the orientation tensors thus obtained are always 1.

Step 8: The θ for which SS is maximum is deemed to be the best alignment between latent and tenprint, and (r^{θ}, c^{θ}) is the point in tenprint where the latent is registered. This (r^{θ}, c^{θ}) corresponds to $(r_m^{\theta}, c_m^{\theta})$ for which SS is maximum.

Step 9: The point (r^{θ}, c^{θ}) is the center of the latent orientation tensor pattern that we have identified in the tenprint, see Fig. 1(g).

Step 10: With (r^{θ}, c^{θ}) as center, and radius as half the diagonal length of the bounding box of latent orientation tensors, we generate a subset of minutiae from the tenprint minutia set which falls inside this circular region, see Fig. 1(h).

V. Experiments

We used the NIST-SD27 database detailed in Section II for the experiments. To register the OF of latent against OF of tenprint images, we used the ideal minutiae dataset from NIST-SD27. The performance of the proposed registration algorithm is measured looking at the percent of the ideal minutiae that we detected in the registered region that is present in the corresponding matched minutia set. We only used the matched dataset (ground truth established by forensic examiner) to check this overlap. The matched minutia sets are a subset of ideal minutia set, but the location and orientation information are not exactly the same. There are slight variations in the location and orientation attributes between ideal and its corresponding matched minutia set originated in the annotations by the experts.

For example, G028T1I and G028T1M of NIST-SD27 contain 123 and 20 minutiae respectively. G028T1I is the ideal minutia set and G028T1M is its corresponding matched minutia set. The pair $(X, Y, Orientation) = (562, 189, -68)$ of ideal and $(564, 182, -73)$ of matched are supposed to be same minutia in the fingerprint. However there is a slight variation with an euclidean distance of 7.2 pixel units. This variation might be because of the uncertainty introduced by the software used by the examiner while generating the matched minutia set. In general, there is a small non-linear deformation between the ideal and matched minutia sets of the tenprints, and we fixed a threshold of 12 pixel units to compensate for this. If the distance between a minutia from ideal and matched sets is less than 12 pixel units, then they are assumed to be corresponding mated pairs. A detailed study on NIST-SD27 where these kind of discrepancies between the ideal and matched minutia sets is reported in [14], where a refined version of the ground truth minutia sets for NIST-SD27 is made publicly available [14].

We perform experiments on Good, Bad and Ugly classifications of NIST-SD27 as detailed in Section II to report the accuracy of the proposed registration algorithm. We also report the rank identification rate for the publicly available Minutia Cylinder-Code (MCC) SDK [1] [15] [16] [17] when incorporating our proposed registration algorithm as a pre-registration before the identification for both minutiae generate OF and image generated OF.

A. Performance measurement protocol

To report the performance of our registration algorithm, we first needed to see how well this algorithm can be utilized as a preprocessing stage to reduce the search space of the minutia in the tenprint for a particular comparison. The registration algorithm finds the subregion in the tenprint that is of the size of bounding box of latent orientation field, together with the rotation parameter that will best align the latent and subregion of tenprint orientation field. The search space of the minutia set in tenprint is now limited to the circular region defined by the size of the latent bounding box (Step 10 in Section IV). The radius of circle is half the length of diagonal centered at the center of bounding box of latent orientation tensors. All minutia of the ideal tenprint that fall inside this circular region become the current search space for latent-tenprint comparison. The search space of the minutiae in tenprint is then reduced to the size of the input latent.

We use the ground truth (otherwise called *matched*) minutia set to check how many of the actual mated minutiae are present in the minutia search space generated by our registration algorithm. If the distance between a minutia from the matched set and the minutia in the search space suggested by our algorithm is less than 12 pixel units, then we conclude that

[1] http://biolab.csr.unibo.it (MCC-SDK Version 1.4)

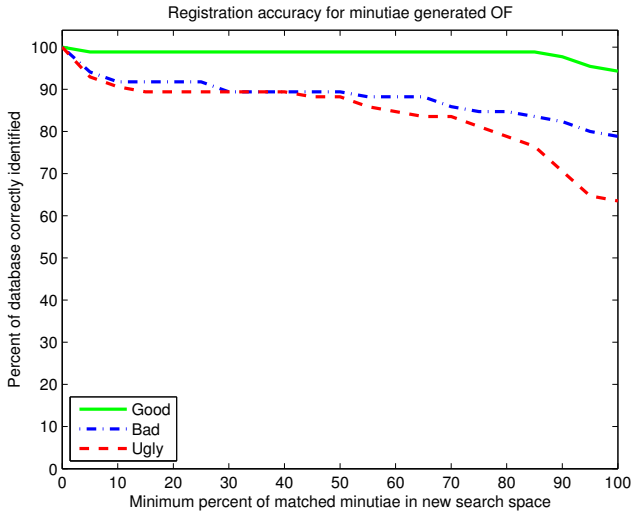

Fig. 2. Registration accuracy for Good, Bad and Ugly quality classification of NIST-SD27 when minutiae generated OF is used.

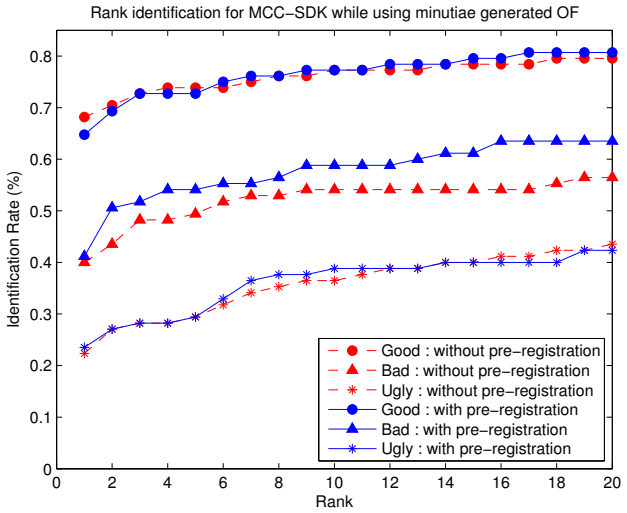

Fig. 4. CMC curve showing the rank identification rate of MCC-SDK with and without pre-registration when minutiae generated OF is used.

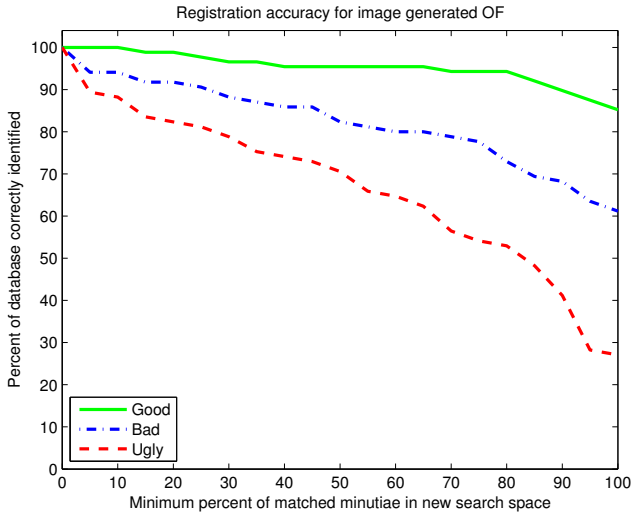

Fig. 3. Registration accuracy for Good, Bad and Ugly quality classification of NIST-SD27 when image generated OF is used.

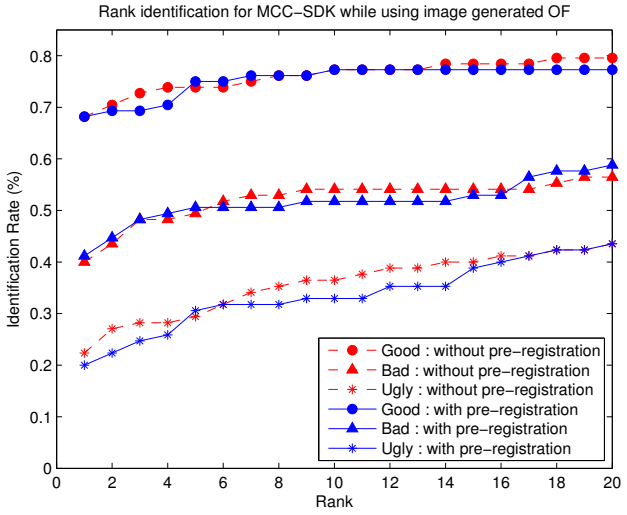

Fig. 5. CMC curve showing the rank identification rate of MCC-SDK with and without pre-registration when image generated OF is used.

a mated pair has been identified by our registration algorithm. This threshold is needed due to the discrepancies of NIST-SD27 database as explained in the beginning of this Section.

B. Experiment 1 : Registration Accuracy

Fig. 2 shows the performance of our registration algorithm on Good, Bad and Ugly classifications datasets of NIST-SD27 using minutiae generated OF. The X-axis is the minimum percent of matched minutiae that should be contained in the reduced minutia search space defined by our algorithm and Y-axis is the percentage of database that satisfies the threshold. For example, if the reduced minutia search space should contain at least 75% of the matched (ground truth) minutiae, then 99% of the database in Good category, 85% of database in Bad category and 82% of database in Ugly category contains 75% or more matched minutiae in the new search space generated by our registration algorithm.

Similarly, Fig. 3 shows the performance of our registration algorithm using image generated OF on Good, Bad and Ugly category. Here, for the same 75% threshold, 95% of database in Good category, 78% of database in Bad category and 55% of database in Ugly category were correctly identified.

C. Experiment 2 : Pre-registration

From the latents, 88 fingerprints of Good category, 85 fingerprints of Bad category and 85 fingerprints of Ugly category were searched in the entire 258 tenprints in the NIST-SD27 database, and their rank identification accuracies before pre-registration and after pre-registration are shown.

Figure 4 shows the CMC curve of MCC-SDK on Good, Bad and Ugly quality classification of NIST-SD27 when minu-

tiae generated OF is used for pre-registration. In case of Bad quality classification, there is a consistent improvement of rank identified rate when pre-registration is incorporated. For Good and Ugly quality category, the rank identification rate improves only slightly.

Figure 5 shows the CMC curve of MCC-SDK on Good, Bad and Ugly quality classification of NIST-SD27 when image generated OF is used for pre-registration. The identification rate in this scenario does not improve mainly because of the quality of the orientation field estimated directly from latent fingerprint images are poor.

As we have observed, the pre-registration helps in improving the identification rate for Good, Bad and Ugly quality categorization when we use minutiae generate orientation field in place of image generated orientation field. Particularly for Bad quality categorization, there is a significant improvement in rank identification rate.

VI. Conclusion and Future Work

Experimental results show that our algorithm can perform the registration based on OF and estimate a subset of minutiae region in tenprint minutiae set for Good, Bad and Ugly quality categorization of NIST-SD27 database. By obtaining such extra information, we can perform pre-registration for any standard minutiae-based matcher by reducing the search space for the matcher. We observed that when we use OF regenerated from minutiae, we are able to achieve better registration accuracy as compared against OF estimated from the latent fingerprint images.

Our registration algorithm used as a pre-registration stage for MCC-SDK, we noticed we were able to improve the rank identification rate for Bad quality category significantly, and slightly for Good and Ugly quality category. This performance is achieved when using OF reconstructed from the minutiae set. This shows the usefulness of our registration algorithm as well the usefulness of minutiae generated OF as compared against image generated OF. Together with the correlation based registration, use of other similarity measures applicable to OF to improve the registration accuracies are under investigation.

Acknowledgment

R.K. was supported by a Marie Curie Fellowship under project BBfor2 (FP7-ITN-238803). This work has also been partially supported by Spanish Guardia Civil, Cátedra UAM-Telefónica, and projects Bio-Shield (TEC2012-34881) and Contexts (S2009/TIC-1485).

References

[1] E. Holder, L. Robinson, and J. Laub, *The Fingerprint Sourcebook*. US Department of Justice, Office of Justice Programs, National Institute of Justice, 2011.

[2] D. Maltoni, D. Maio, A. Jain, and S. Prabhakar, "Handbook of Fingerprint Recognition," *Springer Publishing Company, Incorporated*, 2009.

[3] T. Jea and V. Govindaraju, "A minutia-based partial fingerprint recognition system," *Pattern Recognition*, vol. 38, no. 10, pp. 1672–1684, 2005.

[4] Y. Wang and J. Hu, "Global ridge orientation modeling for partial fingerprint identification," *Pattern Analysis and Machine Intelligence, IEEE Transactions on*, vol. 33, no. 1, pp. 72–87, 2011.

[5] G. Fang, S. Srihari, H. Srinivasan, and P. Phatak, "Use of ridge points in partial fingerprint matching," *Proc. of SPIE: Biometric Technology for Human Identification IV*, pp. 65 390D1–65 390D9, 2007.

[6] A. Jain, Y. Chen, and M. Demirkus, "Pores and ridges: High-resolution fingerprint matching using level 3 features," *Pattern Analysis and Machine Intelligence, IEEE Transactions on*, pp. 15–27, 2007.

[7] J. Feng and A. Jain, "Fingerprint reconstruction: from minutiae to phase," *Pattern Analysis and Machine Intelligence, IEEE Transactions on*, vol. 33, no. 2, pp. 209–223, 2011.

[8] F. Alonso-Fernandez, J. Fierrez, J. Ortega-Garcia, J. Gonzalez-Rodriguez, H. Fronthaler, K. Kollreider, and J. Bigun, "A comparative study of fingerprint image-quality estimation methods," *IEEE Trans. on Information Forensics and Security*, vol. 2, no. 4, pp. 734–743, December 2007.

[9] R. Krish, J. Fierrez, D. Ramos, J. Ortega-Garcia, and J. Bigun, "Partial fingerprint registration for forensics using minutiae-generated orientation fields," in *2nd International Workshop on Biometrics and Forensics*, March 2014.

[10] M. Garris and R. McCabe, "NIST special database 27: Fingerprint minutiae from latent and matching tenprint images," *Technical Report, NISTIR-6534*, 2000.

[11] R. Krish, J. Fierrez, D. Ramos, R. Veldhuis, and R. Wang, "Evaluation of AFIS-ranked latent fingerprint matched template," in *6th Pacific-Aim Symposium on Image and Video Technology*, 2013.

[12] A. Jain and J. Feng, "Latent fingerprint matching," *Pattern Analysis and Machine Intelligence, IEEE Transactions on*, vol. 33, no. 1, pp. 88–100, 2011.

[13] J. Bigun, *Vision with Direction: A Systematic Introduction to Image Processing and Computer Vision*. Springer, 2005.

[14] A. Mikaelyan and J. Bigun, "Ground truth and evaluation for latent fingerprint matching," in *Computer Vision and Pattern Recognition Workshops (CVPRW), 2012 IEEE Computer Society Conference on*. IEEE, 2012, pp. 83–88.

[15] R. Cappelli, M. Ferrara, and D. Maltoni, "Minutia cylinder-code: A new representation and matching technique for fingerprint recognition," *Pattern Analysis and Machine Intelligence, IEEE Transactions on*, vol. 32, no. 12, pp. 2128–2141, 2010.

[16] ——, "Fingerprint indexing based on minutia cylinder-code," *Pattern Analysis and Machine Intelligence, IEEE Transactions on*, vol. 33, no. 5, pp. 1051–1057, 2011.

[17] M. Ferrara, D. Maltoni, and R. Cappelli, "Noninvertible minutia cylinder-code representation," *Information Forensics and Security, IEEE Transactions on*, vol. 7, no. 6, pp. 1727–1737, 2012.